OPEN ACCESS

International
Journal
Of Modern Engineering Research (IJMER)

A Family of Lookup Tables for Novel Vector Controlled Induction Motor Drives

M. Rama Prasad Reddy[1], Dr.B. Brahmaiah[2]

[1]Eee Department, Sri Vasavi Engineering College, Tadepalligudem,, A.P, India

[2]Guntur Engineering College, Guntur, India

ABSTRACT: *This paper presents a family of lookup tables for novel vector controlled induction motor drives. To overcome the drawbacks of vector and direct torque control algorithms, the proposed vector control algorithm combines the principles of both field oriented control (FOC) or vector control and direct torque control (DTC). The proposed vector control algorithm generates the d- and q-axes reference currents by using the principle of classical vector control. Then, by comparing the reference currents and actual currents error current signals are generated. By using the error signals and lookup tables, the suitable voltage vector will be selected based on the principle of DTC. Thus, the proposed algorithm reduces the complexity when compared with the FOC and reduces the steady state torque ripple when compared with the DTC. In this paper, 6, 12 and 24 sector based lookup tables are proposed for the vector control algorithm. To evaluate the proposed lookup tables based vector control algorithms, numerical simulation studies have been carried out and compared. The results show the effectiveness of the proposed algorithms.*

Keywords*: DTC, Induction motor, lookup table, vector control.*

I. INTRODUCTION

Nowadays, the induction motors are becoming popular in variable speed drive (VSD) applications due to less maintenance and low weight volume ratio. So far, many algorithms have been developed for the speed control of induction motor drives. Among the various algorithms, the scalar control, which is also known as volts/hertz control is simple for the implementation. But, the scalar control gives sluggish response due to the coupling effect between the torque and flux. To achieve the decoupling control in induction motor drives similar to that of separately excited dc motor, the field oriented control (FOC), which is also known as vector control has been proposed in [2]. The invention of FOC brought a renaissance in the field of ac drives. Later, so many developments have been proposed for the FOC [3]-[5]. The FOC gives fast transient response due to the decoupled control of torque and flux. Though, the FOC gives good transient response, the complexity involved is more due to the reference frame transformations.

To reduce the complexity involved in FOC, in 1980s, Takahashi proposed direct torque control (DTC) algorithm for induction motor drives [6]. The DTC is simple for the implementation and it directly controls the both torque and flux. It uses two hysteresis comparators for torque and flux loops and a lookup table for the selection of suitable voltage vector. Though, the DTC gives fast dynamic response similar to that of FOC,

it gives large steady state ripple in torque, flux and current. A detailed comparison between FOC and DTC has been discussed in [7]. Moreover, the merits and demerits of FOC and DTC are discussed in detailed.

To reduce the complexity involved in current controlled drives due to the reference frame transformations, a novel algorithm has been proposed in [8] by using the lookup table approach. This approach uses hysteresis comparators and lookup table for the selection of suitable voltage vector. Moreover, a 6-sector and 12-sector based DTC algorithm has been proposed in [9].

Hence, to overcome the drawbacks of conventional vector control algorithm, in this paper novel vector control scheme, which combines the principles of both vector control and DTC, is proposed. The proposed vector control algorithm generates the reference currents by using the principles of FOC. Then, the error current signals have been generated by comparing the reference currents and actual currents.

These error signals will be given to the hysteresis comparators, then the suitable voltage vector is selected by using the principle of DTC. In this paper 6-sector, 12-sector and 24-sector based lookup tables are used for the proposed vector control algorithm.

II. CLASSICAL VECTOR CONTROL

In the vector control algorithm, the decoupling control of torque and flux can be achieved by transferring all the quantities to synchronous reference frame and resolving the stator current vector (i_s^*) as torque producing current component i_{qs}^* and flux producing current component i_{ds}^* . The electromagnetic torque expression for an induction motor is given as

$$T_e = \frac{3}{2}\frac{P}{2}\frac{L_m}{L_r}\left(\psi_{dr} i_{qs} - \psi_{qr} i_{ds}\right) \qquad (1)$$

To achieve decoupled control, i_{ds}^* is oriented along the rotor flux linkage vector, and the i_{qs}^* is normal to the i_{ds}^* . Thus, the entire rotor flux is aligned along d-axis and hence the q-axis flux component will become zero. Then, the modified torque expression can be expressed as given in (2).

$$T_e = \frac{3}{2}\frac{P}{2}\frac{L_m}{L_r}\left(\psi_{dr} i_{qs}\right) \qquad (2)$$

Hence, the rotor flux can be given as $\psi_r = \psi_{dr} = L_m i_{ds}$, which is directly proportional to i_{ds}^* and is maintained constant. Hence, the torque is proportional to the i_{qs}^* . In this paper, the main attention has been focused on indirect vector control algorithm, in which the rotor flux position angle can be calculated from (3).

$$\theta_s = \theta_r + \theta_{sl} = \int \left(\omega_r + \omega_{sl}\right) dt \qquad (3)$$

where $\omega_{sl} = \frac{L_m R_r}{L_r \lambda_r} i_{qs}^*$.

3. Proposed Vector Control

The expression of electromagnetic torque of an induction motor can also be expressed as

$$T_e = \frac{3}{2}\frac{P}{2}\frac{L_m}{L_r}\left|\bar{\lambda}_r\right|\left|\bar{i}_s\right|\sin\delta \qquad (4)$$

where δ is the angle between $\bar{\lambda}_r$ and $\bar{i}_s$. From (4), it can be concluded that the electromagnetic torque can be changed by changing the δ . Hence, fast torque control can be achieved by changing δ in the required manner. Due to the large inertia of rotor circuit, the rotor flux is almost constant for a short time interval. Hence, by changing the stator current vector in the required manner, the torque can be controlled according to the reference torque. By ignoring the stator resistance drop, the stator voltage can be expressed as given in (7).

$$\bar{v}_s = \frac{d\bar{\psi}_s}{dt} \qquad (5)$$

The stator flux linkage space vector of an induction motor can be expressed as in (6)

$$\bar{\psi}_s = L_s \bar{i}_s + \frac{L_m}{L_r}\psi_r - \frac{L_m^2}{L_r}\bar{i}_s \qquad (6)$$

For short time interval, by assuming the ψ_r as constant, the stator voltage expression can be simplified as follows:

$$\bar{v}_s = \frac{d\bar{\psi}_s}{dt} = \left(L_s - \frac{L_m^2}{L_r}\right)\frac{d\bar{i}_s}{dt} = \sigma L_s \frac{d\bar{i}_s}{dt} \qquad (7)$$

where σ is the leakage coefficient of induction motor. From (7), for a short time interval of Δt , the stator current vector can be obtained as

$$\Delta\bar{i}_s = \frac{1}{\sigma L_s}\bar{v}_s \Delta t \qquad (8)$$

Thus, the stator current vector moves by $\Delta\bar{i}_s$ in the direction of the stator voltage vector at a speed proportional to magnitude of voltage vector. By selecting a suitable voltage vector it is then possible to change the stator current in the required manner. Decoupled control can be achieved by acting on the $\bar{i}_{ds}$ and $\bar{i}_{qs}$ components of the stator current vector. The movement of stator current vector can be represented as shown in Fig. 1. This is the basic principle of proposed vector control technique.

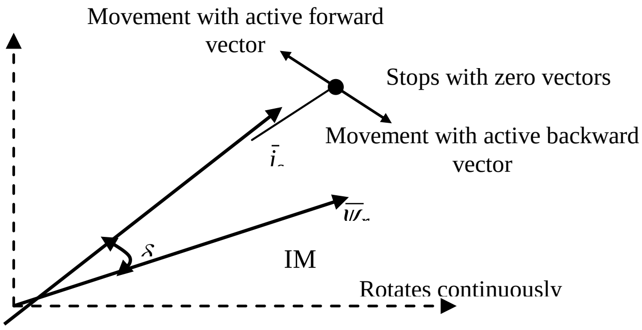

Fig. 1 movement of stator current vector under the influence of voltage vectors

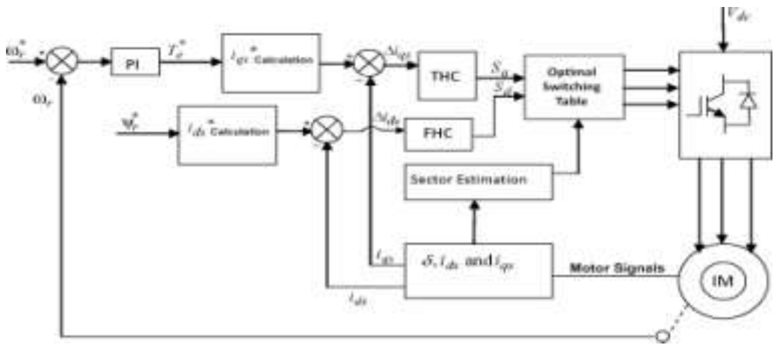

Fig. 2 Block diagram of proposed vector controlled induction motor drive

The block diagram for the proposed vector control algorithm is as shown in Fig. 2. In the proposed control technique, the reference stator current components are at synchronously rotating reference frame. These can be generated by using the principle of classical vector control algorithm. Then, in the proposed control two hysteresis comparators are used for torque and flux control. By using the reference stator current components and actual stator current components, the error current signals are generated. These error current signals will be given to the torque hysteresis comparator (THC) and flux hysteresis comparator(FHC). These hysteresis comparators will generate the digitized outputs based on the error magnitudes. Based on the digitized outputs of the hysteresis comparators and position of the stator current (which will give sector number), the suitable voltage vector are selected so as to maintain the error values within the specified bandwidth of the hysteresis comparators. These selected voltage vectors will be applied to the voltage source inverter fed induction motor drive.

A. 6- Sector Based Vector Control

The possible voltage vectors for a 2-level inverter can be represented as shown in Fig. 3, which consists of six active states and two zero states.

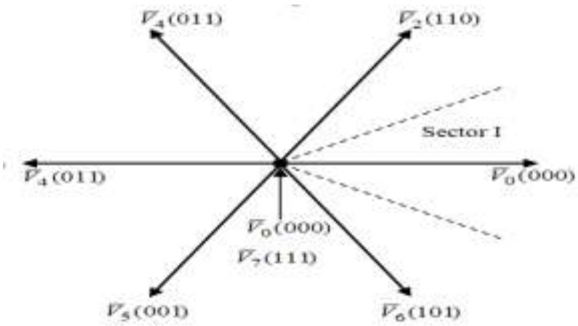

Fig. 3 Possible voltage space vectors for VSI

Based on the position of stator current vector, it is possible to switch the suitable voltage vector to control both $\bar{i}_{ds}$ and $\bar{i}_{qs}$. As the six sectors are symmetrical, in this paper the discussion is limited to the first sector only. When, the $\bar{i}_s$ is in the first sector as shown in Fig.4, then voltage vectors $\overline{V}_2$ and $\overline{V}_6$ can increase the $\bar{i}_{ds}$ and $\overline{V}_3$ and $\overline{V}_5$ can decrease the $\bar{i}_{ds}$. Similarly $\overline{V}_2$ and $\overline{V}_3$ can increase the torque component current $\bar{i}_{qs}$ and $\overline{V}_5$ and $\overline{V}_6$ can decrease the $\bar{i}_{qs}$. Similarly the suitable voltage vectors can be selected for other sectors.

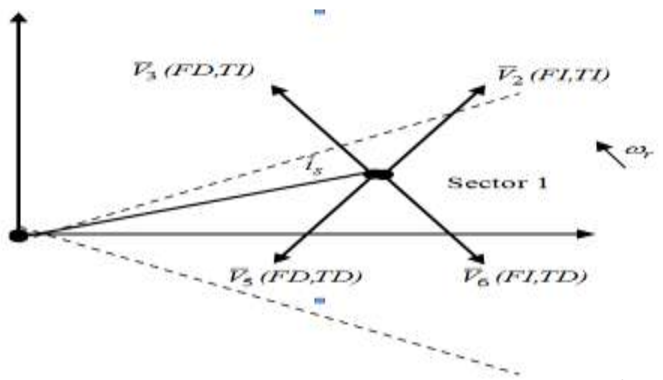

Fig. 4 selection of suitable voltage space vector in sector I (-30^0 to 30^0)

In this method, the current error magnitudes are restricted to $2\Delta\bar{i}_{ds}$ and $2\Delta\bar{i}_{qs}$ within their respective hysteresis bands. In the 6-sector control, a 2-level flux hysteresis and 3-level torque hysteresis comparators are used similar to that of classical DTC algorithm. If increase in $\bar{i}_{ds}$ is required then $S_d = 1$; if decrease in $\bar{i}_{ds}$ is required then $S_d = 0$. Similarly, if increase in $\bar{i}_{qs}$ is required then $S_q = 1$, if decrease in $\bar{i}_{qs}$ is required then $S_q = -1$, and if no change in $\bar{i}_{qs}$ is required then $S_q = 0$. The digital output signals from flux component hysteresis controller (FHC) and torque component hysteresis controller (THC) can be summarized as in Table. 1.

Table. 1 digitized output values of the hysteresis controllers

Controller	Condition	Output of the controller
FHC	$\bar{i}_{ds} \le \bar{i}^*_{ds} - \Delta\bar{i}_s$	$S_d = 1$
	$\bar{i}_{ds} \ge \bar{i}^*_{ds} + \Delta\bar{i}_s$	$S_d = 0$
THC	For anti-clockwise rotation	
	$\bar{i}^*_{qs} - \bar{i}_{qs} \ge \Delta\bar{i}_{qs}$	$S_q = 1$
	$\bar{i}_{qs} \ge \bar{i}^*_{qs}$	$S_q = 0$
	For clockwise rotation	
	$\bar{i}_{qs} \le \bar{i}^*_{qs}$	$S_q = 0$
	$\bar{i}^*_{qs} - \bar{i}_{qs} \le -\Delta\bar{i}_{qs}$	$S_q = -1$

Based on the values of S_d , S_q and the position of the stator current vector, the suitable voltage vector is selected from the lookup table as given in Table. 2.

Table. 2 Optimum voltage vector switching table for 6-sector based vector control

Sector S_d	S_q	I	II	III	IV	V	VI
1	1	$\overline{V}_2$	$\overline{V}_3$	$\overline{V}_4$	$\overline{V}_5$	$\overline{V}_6$	$\overline{V}_1$
	0	$\overline{V}_7$	$\overline{V}_0$	$\overline{V}_7$	$\overline{V}_0$	$\overline{V}_7$	$\overline{V}_0$
	-1	$\overline{V}_6$	$\overline{V}_1$	$\overline{V}_2$	$\overline{V}_3$	$\overline{V}_4$	$\overline{V}_5$
0	1	$\overline{V}_3$	$\overline{V}_4$	$\overline{V}_5$	$\overline{V}_6$	$\overline{V}_1$	$\overline{V}_2$
	0	$\overline{V}_0$	$\overline{V}_7$	$\overline{V}_0$	$\overline{V}_7$	$\overline{V}_0$	$\overline{V}_7$
	-1	$\overline{V}_5$	$\overline{V}_6$	$\overline{V}_1$	$\overline{V}_2$	$\overline{V}_3$	$\overline{V}_4$

B. 12- Sector Based Vector Control

In the 6- sector based vector control, only a limited number of active voltage vectors are used each sector. In order to utilize all six active states in each sector and to reduce the THD further, the space vector plane is divided into twelve sectors instead of six as shown in Fig. 5. However, it is necessary to define small and large variations. It is observed that V_1 will produce a large increase in flux and a small increase in torque in sector-12. On the other hand it is observed that V_2 will produce a large increment in torque and a small increment in flux. The proposed 12-sector based vector control uses a four level torque hysteresis controller (TI: torque increase, TSI: torque small increase, TD: torque decrease and TSD: torque small decrease) and a two level flux hysteresis controller. The look-up table for 12-sector based FOC is presented in Table 3.

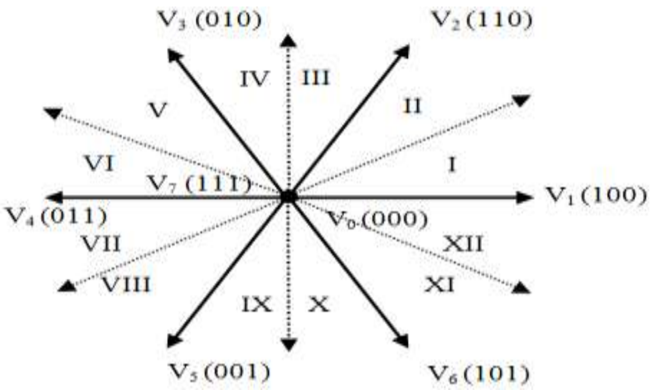

Fig. 5 Possible voltage space vectors for VSI in 12- sector based vector control algorithm

Table. 3 Optimum voltage vector switching table for 12-sector based vector control

S_d	S_q	S_1	S_2	S_3	S_4	S_5	S_6	S_7	S_8	S_9	S_{10}	S_{11}	S_{12}
1	TI	$\overline{V}_2$	$\overline{V}_3$	$\overline{V}_3$	$\overline{V}_4$	$\overline{V}_4$	$\overline{V}_5$	$\overline{V}_5$	$\overline{V}_6$	$\overline{V}_6$	$\overline{V}_1$	$\overline{V}_1$	$\overline{V}_2$
	TsI	$\overline{V}_2$	$\overline{V}_2$	$\overline{V}_3$	$\overline{V}_3$	$\overline{V}_4$	$\overline{V}_4$	$\overline{V}_5$	$\overline{V}_5$	$\overline{V}_6$	$\overline{V}_6$	$\overline{V}_1$	$\overline{V}_1$
	TsD	$\overline{V}_1$	$\overline{V}_1$	$\overline{V}_2$	$\overline{V}_2$	$\overline{V}_3$	$\overline{V}_3$	$\overline{V}_4$	$\overline{V}_4$	$\overline{V}_5$	$\overline{V}_5$	$\overline{V}_6$	$\overline{V}_6$
	TD	$\overline{V}_6$	$\overline{V}_1$	$\overline{V}_1$	$\overline{V}_2$	$\overline{V}_2$	$\overline{V}_3$	$\overline{V}_3$	$\overline{V}_4$	$\overline{V}_4$	$\overline{V}_5$	$\overline{V}_5$	$\overline{V}_6$
0	TI	$\overline{V}_3$	$\overline{V}_4$	$\overline{V}_4$	$\overline{V}_5$	$\overline{V}_5$	$\overline{V}_6$	$\overline{V}_6$	$\overline{V}_1$	$\overline{V}_1$	$\overline{V}_2$	$\overline{V}_2$	$\overline{V}_3$
	TsI	$\overline{V}_4$	$\overline{V}_4$	$\overline{V}_5$	$\overline{V}_5$	$\overline{V}_6$	$\overline{V}_6$	$\overline{V}_1$	$\overline{V}_1$	$\overline{V}_2$	$\overline{V}_2$	$\overline{V}_3$	$\overline{V}_3$
	TsD	$\overline{V}_7$	$\overline{V}_5$	$\overline{V}_0$	$\overline{V}_6$	$\overline{V}_7$	$\overline{V}_1$	$\overline{V}_0$	$\overline{V}_2$	$\overline{V}_7$	$\overline{V}_3$	$\overline{V}_0$	$\overline{V}_4$
	TD	$\overline{V}_5$	$\overline{V}_6$	$\overline{V}_6$	$\overline{V}_1$	$\overline{V}_1$	$\overline{V}_2$	$\overline{V}_2$	$\overline{V}_3$	$\overline{V}_3$	$\overline{V}_4$	$\overline{V}_4$	$\overline{V}_5$

C. 24- Sector Based Vector Control

To reduce the THD further, in this paper a 24-sector based vector control algorithm has been proposed. In this method the space vector plane is divided into 24 sectors as shown in Fig. 6. In this method, similar to the 6-sector based control technique, the current error magnitudes are restricted to

$2\Delta\bar{i}_{ds}$ and $2\Delta\bar{i}_{qs}$ within their respective hysteresis bands. In the 24-sector control, 3-level hysteresis controllers are used for d- and q-axes current controllers. The operation of the 3-level hysteresis controller is similar to that of q-axis current controller of 6-sector based vector control algorithm.

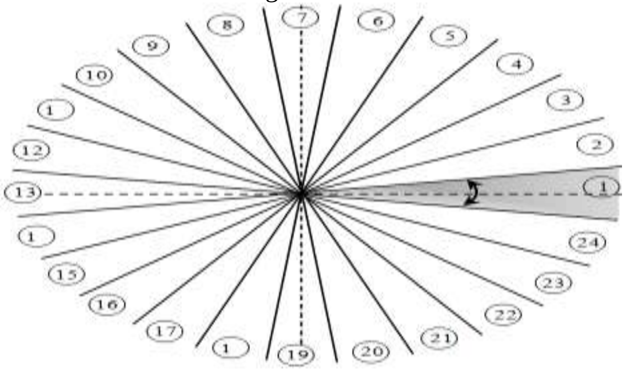

Fig. 6 Possible voltage space vectors for VSI in 24- sector based vector control algorithm

The digital output signals from flux component hysteresis controller (FHC) and torque component hysteresis controller (THC) can be summarized as in Table. 4.

Table.4 digitized output values of the hysteresis controllers

Controller	Condition	Output of the controller
FHC	For anti-clockwise rotation	
	$\bar{i}_{ds}^{*} - \bar{i}_{ds} \geq \Delta\bar{i}_{ds}$	$S_q = 1$
	$\bar{i}_{ds} \geq \bar{i}_{ds}^{*}$	$S_q = 0$
	For clockwise rotation	
	$\bar{i}_{ds} \leq \bar{i}_{ds}^{*}$	$S_q = 0$
	$\bar{i}_{ds}^{*} - \bar{i}_{ds} \leq -\Delta\bar{i}_{ds}$	$S_q = -1$
THC	For anti-clockwise rotation	
	$\bar{i}_{qs}^{*} - \bar{i}_{qs} \geq \Delta\bar{i}_{qs}$	$S_q = 1$
	$\bar{i}_{qs} \geq \bar{i}_{qs}^{*}$	$S_q = 0$
	For clockwise rotation	
	$\bar{i}_{qs} \leq \bar{i}_{qs}^{*}$	$S_q = 0$
	$\bar{i}_{qs}^{*} - \bar{i}_{qs} \leq -\Delta\bar{i}_{qs}$	$S_q = -1$

Based on the values of S_d , S_q and sector number, the suitable voltage vector is selected from the lookup table as given in Table. 5.

Table. 5 Optimum voltage vector switching table for 24-sector based vector control

Sector d_x	d_y	1	2	3	4	5	6	7	8	9	10	11	12	13	14	15	16	17	18	19	20	21	22	23	24
1	1	V_2	V_2	V_2	V_3	V_3	V_3	V_3	V_4	V_4	V_4	V_4	V_5	V_5	V_5	V_5	V_6	V_6	V_6	V_6	V_1	V_1	V_1	V_1	V_2
1	0	V_1	V_1	V_2	V_2	V_2	V_2	V_3	V_3	V_3	V_3	V_4	V_4	V_4	V_4	V_5	V_5	V_5	V_5	V_6	V_6	V_6	V_6	V_1	V_1
1	-1	V_6	V_1	V_1	V_1	V_1	V_2	V_2	V_2	V_2	V_3	V_3	V_3	V_3	V_4	V_4	V_4	V_4	V_5	V_5	V_5	V_5	V_6	V_6	V_6
0	1	V_3	V_3	V_3	V_3	V_4	V_4	V_4	V_4	V_5	V_5	V_5	V_5	V_6	V_6	V_6	V_6	V_1	V_1	V_1	V_1	V_2	V_2	V_2	V_2
0	0	V_0	V_0	V_0	V_0	V_0	V_0	V_0	V_0	V_0	V_0	V_0	V_0	V_0	V_0	V_0	V_0	V_0	V_0	V_0	V_0	V_0	V_0	V_0	V_0
0	-1	V_6	V_6	V_6	V_6	V_1	V_1	V_1	V_1	V_2	V_2	V_2	V_2	V_3	V_3	V_3	V_3	V_4	V_4	V_4	V_4	V_5	V_5	V_5	V_5
-1	1	V_3	V_4	V_4	V_4	V_4	V_5	V_5	V_5	V_5	V_6	V_6	V_6	V_6	V_1	V_1	V_1	V_1	V_1	V_1	V_2	V_2	V_2	V_2	V_3

-1	0	V_4	V_4	V_5	V_5	V_5	V_5	V_6	V_6	V_6	V_6	V_1	V_1	V_1	V_1	V_2	V_2	V_2	V_2	V_3	V_3	V_3	V_3	V_4	V_4
-1	-1	V_5	V_5	V_5	V_6	V_6	V_6	V_6	V_1	V_1	V_1	V_1	V_2	V_2	V_2	V_2	V_3	V_3	V_3	V_3	V_4	V_4	V_4	V_4	V_5

SIMULATION RESULTS AND DISCUSSION

To validate the proposed lookup tables based vector control algorithm numerical simulation studies have been carried out by using MATLAB. For the simulation studies the motor parameters are taken as R_s =1.57Ω, R_r=1.21 Ω, L_m=0.165H, L_s=0.17H, L_r=0.17H and J=0.089 Kg-m^2. Moreover, for the simulation results equal band widths have been considered for the hysteresis bands in the proposed and existing current controlled vector controlled drives. The simulation results of classical vector controlled induction motor drive are shown in Fig.7-Fig.12. The simulation results of 6 sector based vector controlled induction motor drive are given from Fig. 13 to Fig. 18. The simulation results for 12 sector based vector controlled drive are given from Fig. 19 to Fig. 24 and the simulation results of 24-sector based vector control algorithm are shown in Fig. 25-Fig.30.

From the simulation results, it can be observed that the proposed lookup table based vector control algorithms give fast transient response like conventional vector control algorithm. Also, it can be observed that the 6 - Sector algorithm gives less total harmonic distortion (THD) value when compared with the conventional vector control algorithm for same band width of the hysteresis controllers. Moreover, the 6-sector based vector control algorithm gives fixed switching frequency operation when compared with the classical vector control algorithm, which can be observed from the line voltage.

To reduce the THD further, a 12 sector and 24 sector lookup tables based vector control algorithms are proposed in this paper. From the steady state simulation results and harmonic spectra of line currents, it can be observed that the proposed 24 sector lookup table based vector control algorithm gives reduced harmonic distortion when compared with the other control algorithms.

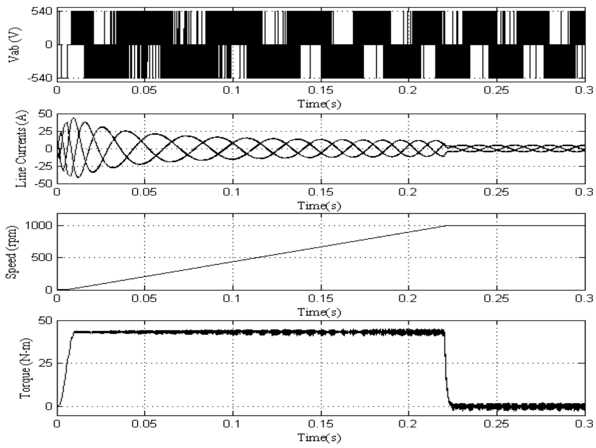

Fig. 7 starting transients of classical vector control algorithm based induction motor drive

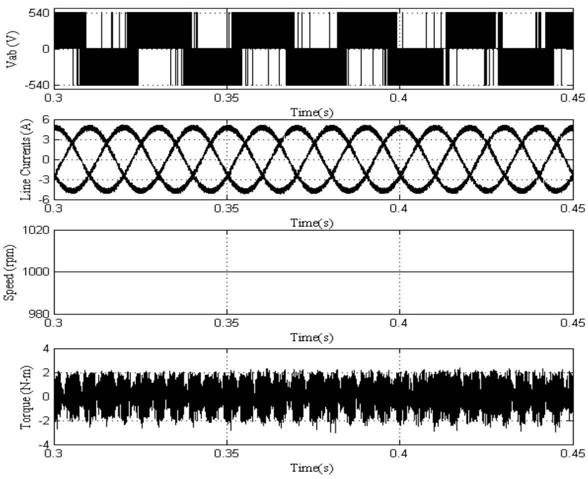

Fig. 8 steady state plots of classical vector control algorithm based induction motor drive

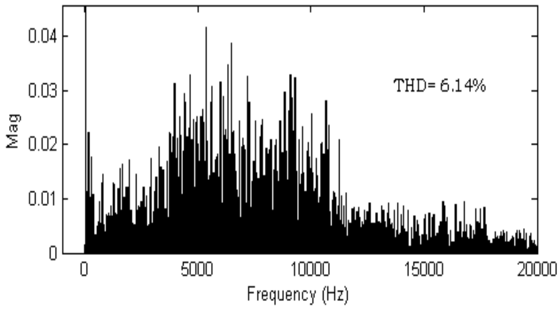

Fig. 9 Harmonic spectra of stator current in classical vector control algorithm

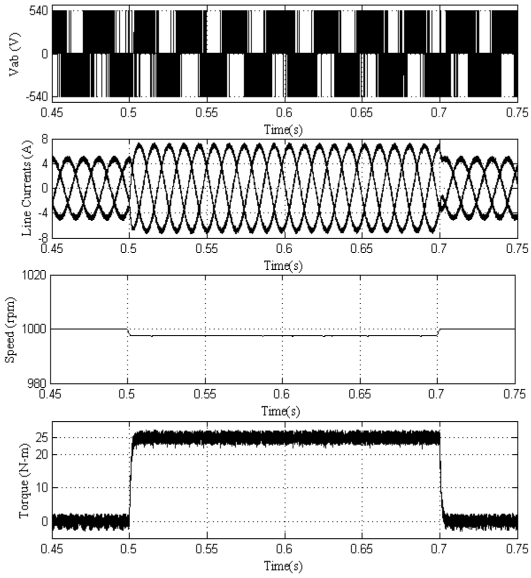

Fig. 10 Transients during the step change in load (a 25 N-m load is applied at 0.5 sec and removed at 0.7 sec) for classical vector control algorithm based induction motor drive

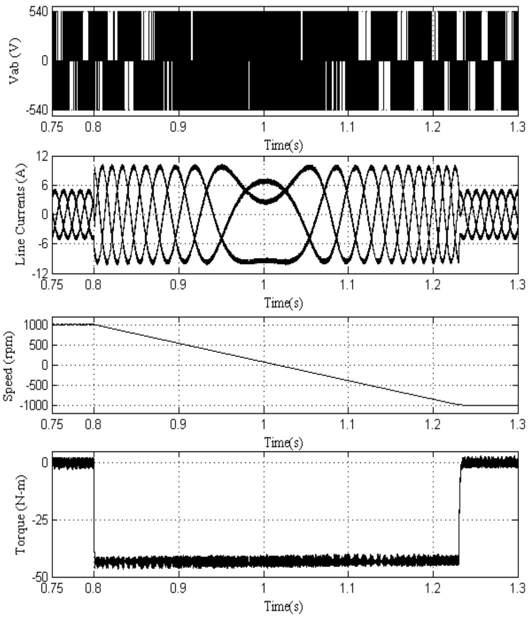

Fig. 11 Transients during the speed reversal (from +1000 rpm to -1000 rpm) for classical vector control algorithm based induction motor drive

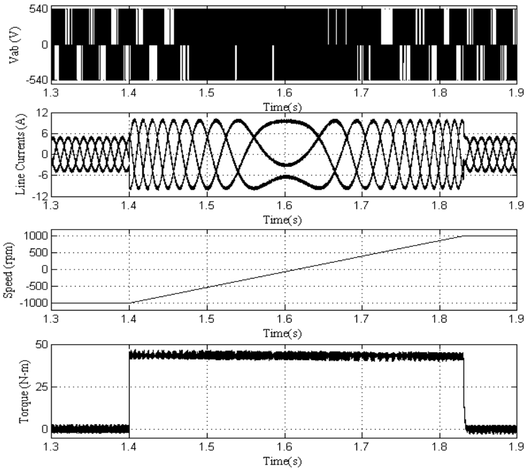

Fig. 12 Transients during the speed reversal (from -1000 rpm to +1000 rpm) for classical vector control algorithm based induction motor drive

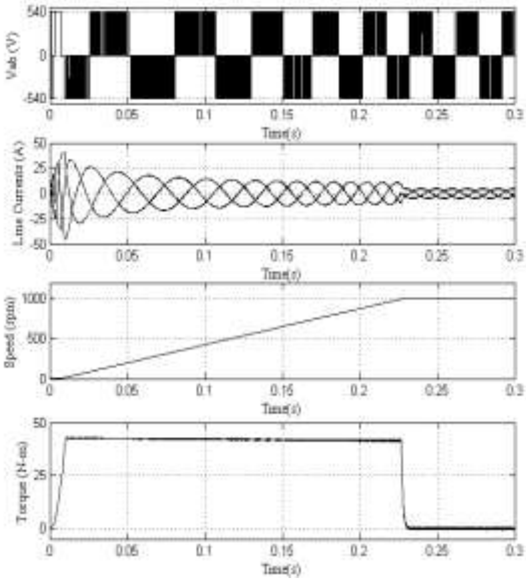

Fig. 13 starting transients of 6 - Sector algorithm vector control algorithm based induction motor drive

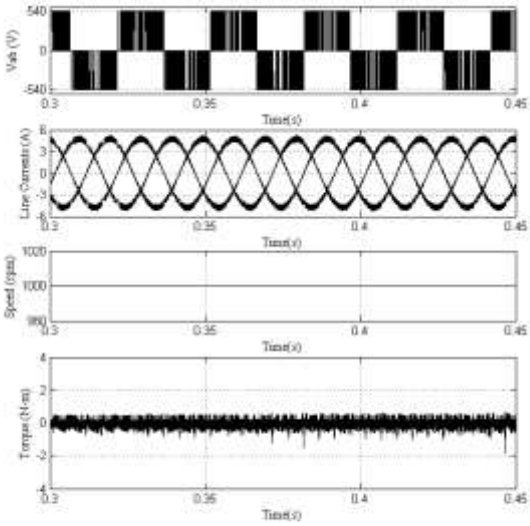

Fig. 14 steady state plots of 6 - Sector algorithm vector control algorithm based induction motor drive

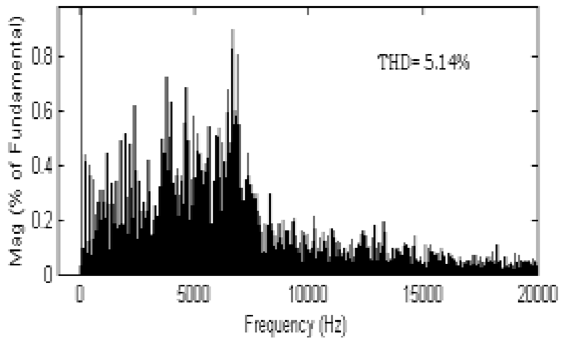

Fig. 15 Harmonic spectra of stator current in 6 - Sector algorithm vector control algorithm based induction motor drive

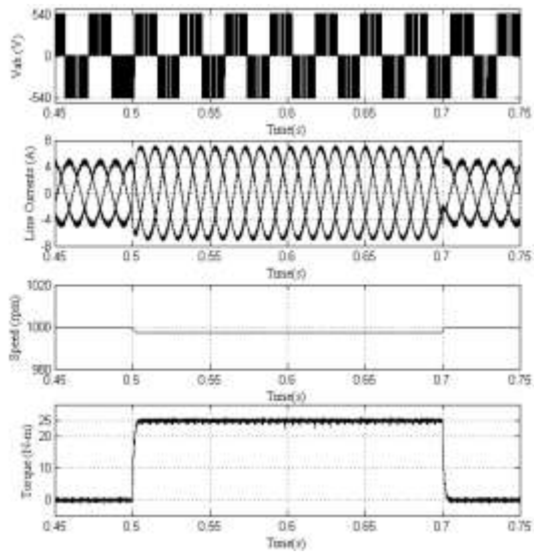

Fig. 16 Transients during the step change in load (a 25 N-m load is applied at 0.5 sec and removed at 0.7 sec) for 6 - Sector algorithm vector control algorithm based induction motor drive

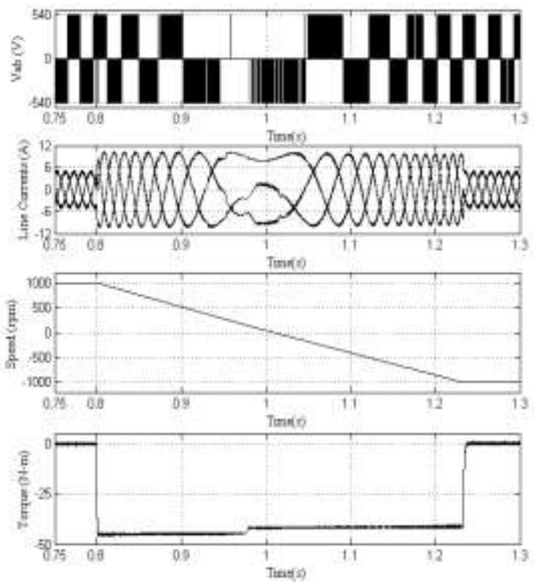

Fig. 17 Transients during the speed reversal (from +1000 rpm to -1000 rpm) for 6 - Sector algorithm vector control algorithm based induction motor drive

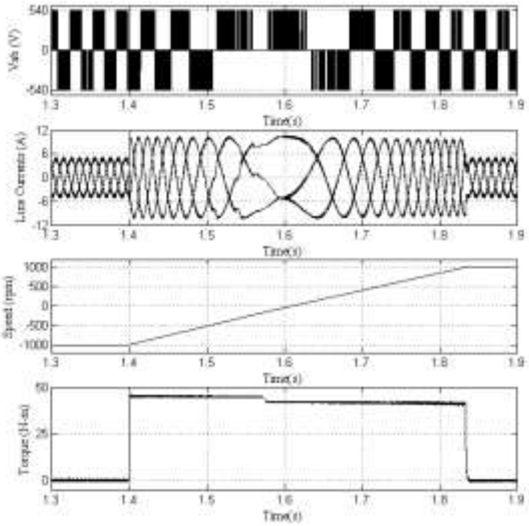

Fig. 18 Transients during the speed reversal (from -1000 rpm to +1000 rpm) for 6 - Sector algorithm vector control algorithm based induction motor drive

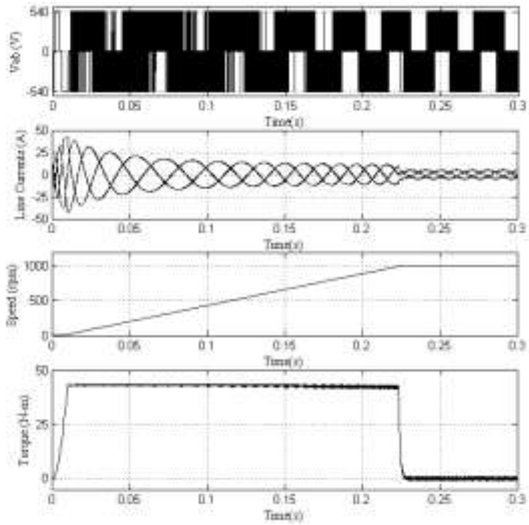

Fig. 19 starting transients of proposed 12 - Sector algorithm based vector controlled induction motor drive

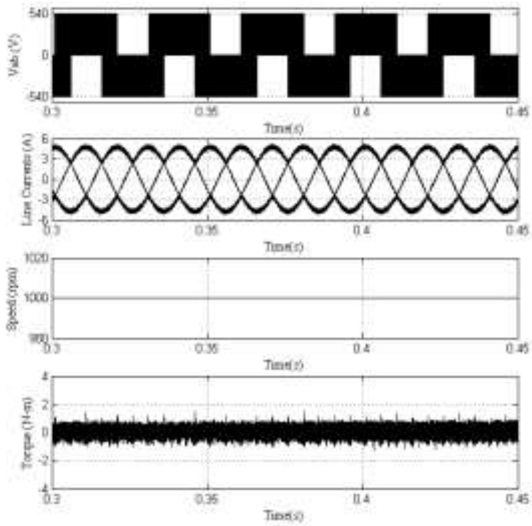

Fig. 20 steady state plots of proposed 12 - Sector algorithm based vector controlled induction motor drive

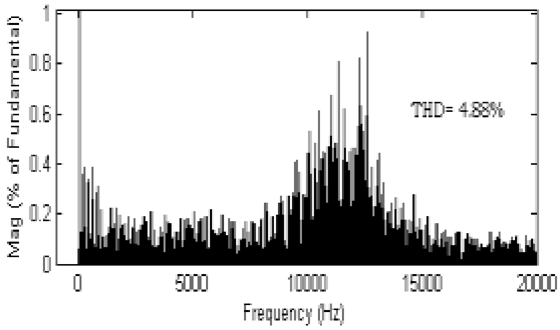

Fig. 21 Harmonic spectra of stator current in proposed 12 - Sector algorithm based vector controlled induction motor drive

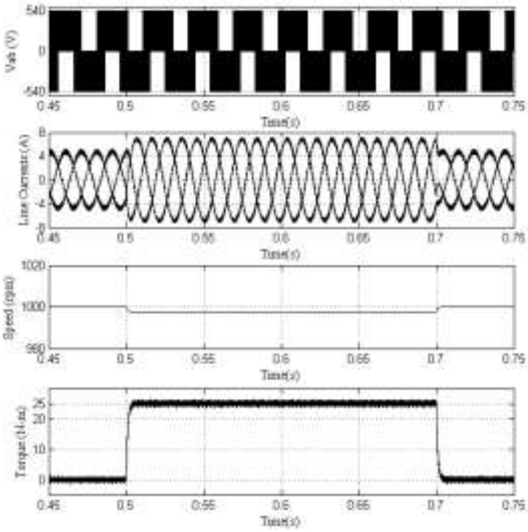

Fig. 22 Transients during the step change in load (a 25 N-m load is applied at 0.5 sec and removed at 0.7 sec) for proposed 12 - Sector algorithm based vector controlled induction motor drive

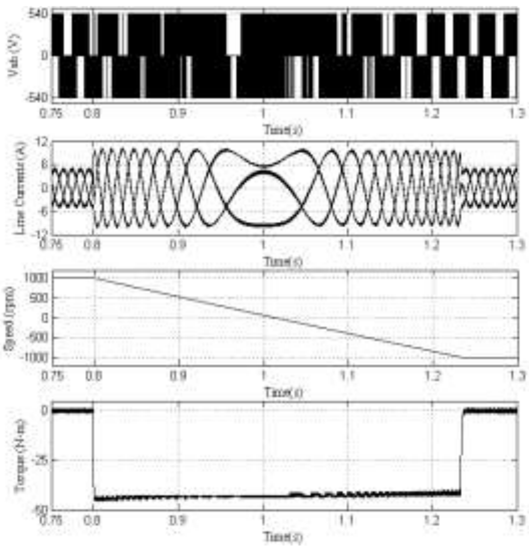

Fig. 23 Transients during the speed reversal (from +1000 rpm to -1000 rpm) for proposed 12 - Sector algorithm based vector controlled induction motor drive

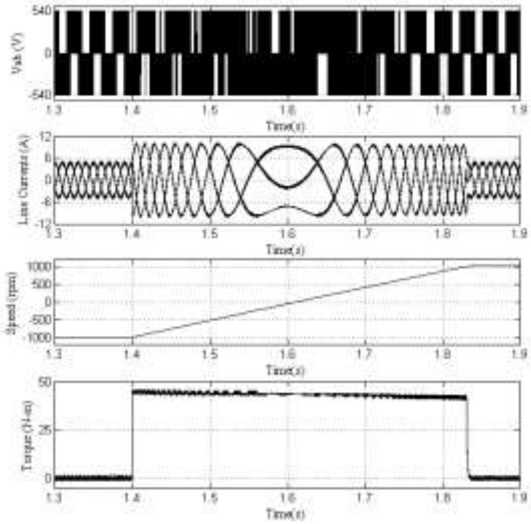

Fig. 24 Transients during the speed reversal (from -1000 rpm to +1000 rpm) for proposed 12 - Sector algorithm based vector controlled induction motor drive

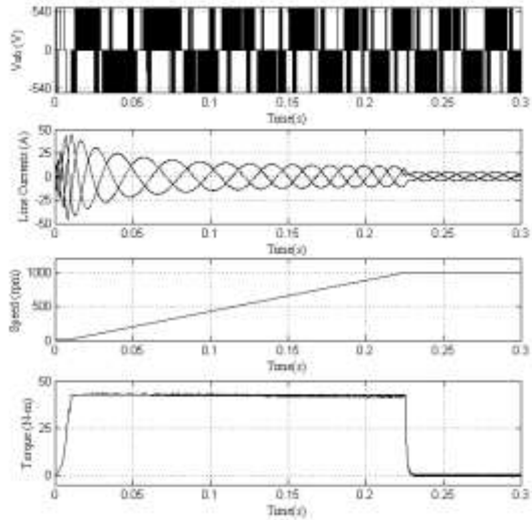

Fig. 25 starting transients of proposed 24 - Sector algorithm based vector controlled induction motor drive

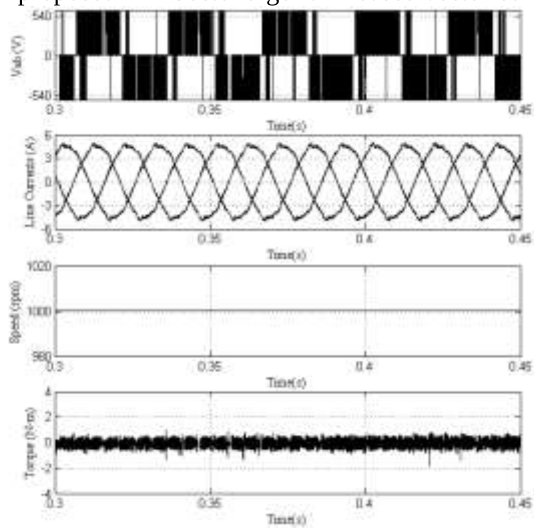

Fig. 26 steady state plots of proposed 24 - Sector algorithm based vector controlled induction motor drive

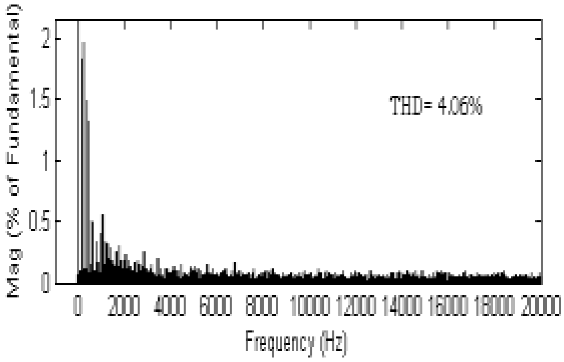

Fig. 27 Harmonic spectra of stator current in proposed 24 - Sector algorithm based vector controlled induction motor drive

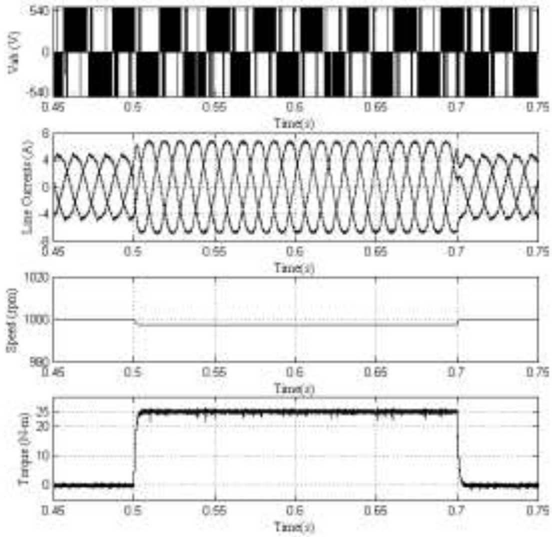

Fig. 28 Transients during the step change in load (a 25 N-m load is applied at 0.5 sec and removed at 0.7 sec) for proposed 24 - Sector algorithm based vector controlled induction motor drive

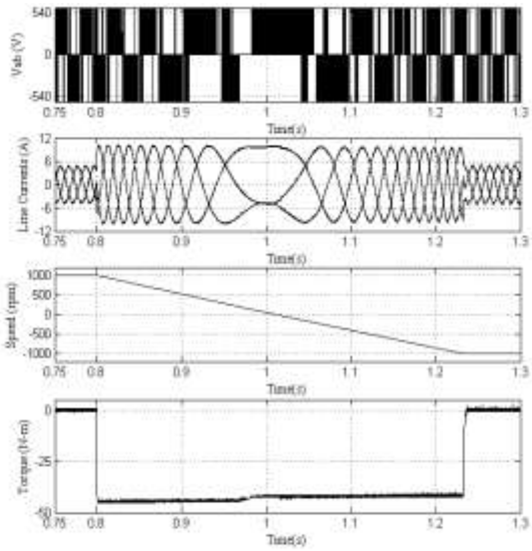

Fig. 29 Transients during the speed reversal (from +1000 rpm to -1000 rpm) for proposed 24 - Sector algorithm based vector controlled induction motor drive

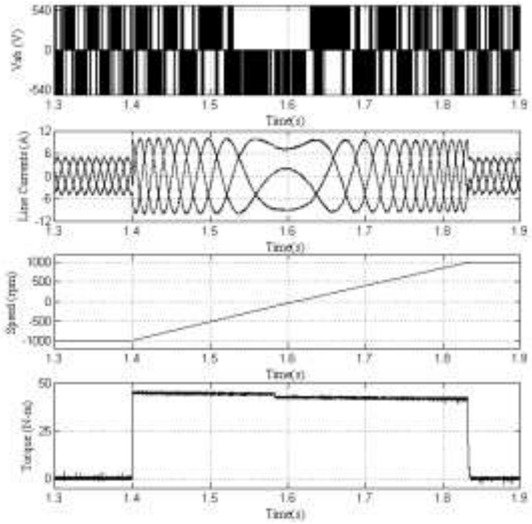

Fig. 30 Transients during the speed reversal (from -1000 rpm to +1000 rpm) for proposed 24 - Sector algorithm based vector controlled induction motor drive

V. CONCLUSIONS

The vector controlled induction motor drives are becoming popular in variable speed drive applications. Though, the classical vector control algorithm gives fast transient response, the complexity involved is more due to the reference frame transformations. Hence, to reduce the complexity, a novel vector control algorithm is presented in this paper, which combines the principles of both vector control and direct torque control. The proposed control uses hysteresis comparators and lookup tables. To show the effectiveness of the proposed lookup tables based vector control algorithm, several simulation results are presented and compared. From the simulation results, it can be observed that the proposed lookup tables based vector control gives good transient response with reduced harmonic distortion and complexity when compared with the classical vector control algorithm.

REFERENCES

[1]. R.Ueda and T. Sonada K Koga and M. Ichikawar "stability analysis of induction motor drives by V/f control by general purpose inverter" IEEE Trans.Ind.Appl .vol.28.PP 472-481.March/april 1992.

[2]. F. Blaschke “The principle of field orientation as applied to the new transvector closed loop control system for rotating-field machines," Siemens Review, 1972, pp 217-220.

[3]. Isao Takahashi, Toshihiko Noguchi, “A new quick response and high-efficiency control strategy of an induction motor”, IEEE Trans Ind Appl, Vol.IA-22, No.5, pp. 820-827, Sep/Oct, 1986.

[4]. W. Leonhard, “30 years of space vectors, 20 years of field orientation, 10 years of digital signal processing with controlled AC-drives, a review (Part1)". EPE Journal, No. 1, July 1991, pages 13-20.

[5]. W. Leonhard, “30 years of space vectors, 20 years of field orientation, 10 years of digital signal processing with controlled AC-drives, a review (Part 2)". EPE Journal, No. 2, Oct, 1991, pages 89-102.

[6]. J. A. Santisteban, and R. M. Stephan, “Vector control methods for induction machines: an overview,” IEEE Trans. On Education, vol. 44, no. 2, pp. 170-175, May 2001.

[7]. Domenico Casadei, Francesco Profumo, Giovanni Serra, and Angelo Tani, “FOC and DTC: Two Viable Schemes for Induction Motors Torque Control” IEEE Trans. Power Electron., vol. 17, no.5, Sep, 2002, pp. 779-787.

[8]. Marian P. Kaimierkowski, Maciej A. Dzieniakowski, and Waldemar Sulkowski, “Novel Space Vector Based current controllers for PWM-inverters” IEEE Trans. Power Electronics, vol.6, no.1, Jan, 1991, pp. 158-166.

[9]. Y.V.Siva Reddy, M.Vijayakumar and T. Brahmananda Reddy, “Direct Torque Control of Induction Motor Using Sophisticated Lookup Tables Based on Neural Networks” AIML Journal, Volume (7), Issue (1), June, 2007, pp. 9-15.

[10]. L. Zarri, Senior Member, IEEE, M. Mengoni, Member, IEEE, A. Tani,G. Serra, Senior Member, IEEE, D. Casadei, Fellow, IEEE, and J. O. Ojo, Fellow, IEEE.

[11]. “Control Schemes for Field Weakening of Induction Machines: a Review” 978-1-4799-8900-3/15/$31.00 ©2015 IEEE.

[12]. Y. Agrebi Zorgani, Y. Koubaa, M. Boussak, Senior Member, IEEE. “Sensorless Speed Control with

[13]. MRAS for Induction Motor Drive" 978-1-4673-0142- 8/12/$26.00 ©2012 IEEE.
[14]. Abhijit Choudhury and Kishore Chatterjee, "Speed Sensor Less Direct Torque Controlled Induction Motor Drive with Constant Switching Frequency Operation" 978-1-4577-0776-6/11/$26.00 ©2011 IEEE.
[15]. Kang Jinsong, Chen Yu, Wan Haifeng, Niu Yichuan ,"Three-level Inverter Speed Sensorless System with Field Orientation Control," 2012 IEEE 7th International Power Electronics and Motion Control Conference - ECCE Asia.
[16]. Edison Roberto C. Da Silva, Euzeli Cipriano Dos Santos Jr, and Cursion Branda O Jacobina, "Pulse width
[17]. modulation strategies" IEEE Ind.Electronics Magazine, pp. 37-45, Jun, 2011.
[18]. Mansour Mohseni, and Syed M. Islam, "A New Vector- Based Hysteresis Current Control Scheme for Three- Phase PWM Voltage-Source Inverters" IEEE Trans. on Power Electron., vol. 25, no.9, Sep, 2010, pp. 2299-2309.

Biographies

Dr.M.Rama Prasad Reddy received the Bachelor of Engineering degree in Electrical & Electronics Engineering from Karnataka University of Dharwad in 1999 and Master's degree from JNTU Kakinada in 2007. He is recently completed Doctoral degree from JNTU, Hyderabad. Currently, working as an Associate Professor in Sri Vasavi Engineering College, Tadepalligudem, A.P. His areas of interests are in power systems, Power electronic control of drives.

Dr. B.Brahmaiah received the Bachelor of Technology degree in Electrical & Electronics Engineering from JNTU, Hyderabad in 1979, and Master's degree from National Institute of Technology, Warangal in 1982 and Ph.D from JNTU, Hyderabad in 2001. He is presently working as Principal of Guntur Engineering College,Guntur. He presented many research papers in various national and international journals and conferences. His researches areas include are in Electrical Machines and Power Electronic Drives.